

Received February 25, 2022, accepted March 4, 2022, date of publication March 14, 2022, date of current version March 25, 2022.

Digital Object Identifier 10.1109/ACCESS.2022.3159333

A Skid-Steering Method for Path-Following Control of Distributed-Drive Articulated Heavy Vehicles

FANG YANG^{1,2}, XUANHAO CAO^{1,3}, TAO XU^{1,3}, AND XUEWU JI³

¹Postdoctoral Research Center of Agricultural Bank of China, Beijing 100005, China

²School of Economics, Peking University, Beijing 100091, China

³State Key Laboratory of Automotive Safety and Energy, Tsinghua University, Beijing 100084, China

Corresponding author: Tao Xu (ustb_xt@163.com)


This work was supported in part by the National Natural Science Foundation of China under Grant 52104163, and in part by the Foundation of State Key Laboratory of Automotive Simulation and Control under Grant 20210232.

ABSTRACT Distributed-drive articulated heavy vehicles (DAHVs) have separate front and rear sections and require a complex hydraulic steering system to achieve the steering process, which poses considerable challenges in obtaining better steering characteristics and achieving path-following control. In this paper, the distributed-drive characteristic of DAHVs is used to develop a novel skid-steering method (SSM) in which the hydraulic steering method (HSM) is replaced with a system that differentially controls the driving wheels to improve vehicle steering performance and path following control accuracy. Three main contributions are made: 1) The novel SSM with direct yaw moment that is used to be the sole power source during steering process of DAHVs is designed to replace the conventional HSM. 2) The idea of SSM by yaw rate control of one vehicle section to achieve the steering process for DAHVs is proposed firstly, which can solve the complex problem of requiring multiple control parameters due to the separate vehicle sections of DAHVs. 3) A layered control method is implemented to improve the robustness of the control system, which is composed of an upper path following controller and a lower skid steering controller combined with a double sliding mode control technique. The system's stability and robustness are proven by the Lyapunov approach. A co-simulation model verified by field tests is used to demonstrate the feasibility and effectiveness of the proposed control method. The results of this study provide a new way to improve the intelligence of DAHVs.

INDEX TERMS Distributed-drive articulated vehicle, hydraulic steering method, skid steering method, sliding mode control.

I. INTRODUCTION

Automated driving technology for passenger cars and heavy commercial vehicles has become an important research direction in both academia and industry [1]–[3]. However, previous researches on the intelligent control of distributed articulated heavy vehicles (DAHVs) is inadequate, especially regarding path following control methods [4], [5]. Although research on automated DAHV driving commenced after that on passenger cars and heavy commercial vehicles, it is believed that DAHVs may be the first to become fully automated as they are used in unmanned working environments with fixed working routes that require low driving

The associate editor coordinating the review of this manuscript and approving it for publication was Tao Wang .

speeds [6], [7]. Therefore, further researches on path-following control technology for DAHVs is needed.

The structure of DAHVs is special because they use two independent sections connected by two hydraulic cylinders and an articulated joint without a locking mechanism [8]–[10]. Their front and rear parts can rotate relative to each other, which complicates its dynamic analysis. Moreover, the complex hydraulic steering system is entrained with gas and is prone to leaking, which can decrease the vehicle's torsional stiffness and increase oscillatory yaw motions that lead to instability [11], [12]. Existing research has not provided good solutions to these problems. Therefore, this paper considers the characteristics of the independent driving wheels of DAHVs to design a novel skid steering method (SSM) that can replace conventional hydraulic

steering method (HSM) and then verifies the resulting path-following performance.

The SSM is a novel steering method that does not depend on mechanical systems. It is very suited to DAHVs due to its two independent agent systems with wheel-side motors [13], [14]. In previous research, SSM has always been used as assisted steering power to improve the vehicle's yaw stability [15] or decrease its turning radius [16] without changing the original structure of the HSM. In fact, SSM can be used as the sole power source during steering with the HSM removed from the DAHV. However, there is a need to provide coordinated control for the relatively independent agent system of DHAVs and there is little research on SSMs with yaw moment control for DAHVs.

Moreover, there is no research on path-following control methods based on SSM for DAHVs. Most existing research has used an HSM as the basic structure in DAHVs and referred to path-following processes in conventional vehicles, such as PID control, sliding mode control (SMC) [17], [18], non-linear model predictive control (NMPC) [19], linear time-varying predictive control [20], and robust H_∞ control [21]. Studies on automated path tracking control for AAHVs remain inadequate. Astolfi *et al.* [22] presented a Lyapunov technique to address the problem of asymptotic stabilization for backward motion of AAHVs during path-tracking processes. Nayl *et al.* [23] proposed a control architecture to improve the performance of vehicle path tracking. It consists of a switching control scheme based on a model predictive control strategy that considers variations in vehicle velocity and slip angle. Gao *et al.* [4] used the dynamic virtual terrain field method to achieve path-tracking control for articulated-steering vehicles. Although these studies achieved path following control, they are not suitable for DAHVs with SSMs. Therefore, more research is needed to improve the path-tracking performance of DAHVs with SSMs.

This paper aims to provide a layered control framework for the path-following control of DAHVs based on a novel skid-steering method. Firstly, a method is proposed to use SSM as the sole power source to control the yaw rate of the front vehicle section to achieve steering control in DAHVs. This method solves the problem of the collaborative control of DAHVs with two independent sections. Moreover, a layered control framework with the double sliding mode control (DSMC) method is developed to achieve path-following control for DAHVs with SSMs. The stability and robustness of the controller are proven via the Lyapunov approach. A co-simulation model is implemented to verify the effectiveness of the proposed control method.

The remainder of this paper is organized as follows: Section II presents a dynamic model for DAHVs. In Section III, a skid-steering controller and path-following controller are proposed. Section IV presents the results of simulations of the path-following and skid-steering processes for DAHVs under different driving conditions. Conclusions and future research prospects are summarized in Section V.

II. DYNAMIC MODELLING OF DAHVS

This section presents a dynamic model of DAHVs that considers lateral and yaw motions. A schematic diagram of the vehicle dynamic model, which considers the skid steering and path-tracking processes, is shown in Fig.1. In conventional DAHV design, there is no suspension in the chassis system. The vertical, roll and pitch motions of the vehicle and their effects on vehicle steering can be neglected. Moreover, the hydraulic steering system is simplified as a spring-damp system ($k_\theta - C_\theta$) to represent the compressibility effects and friction in the hydraulic struts and articulation joint [15], [24]. The articulation joint is simplified as a hinge. In this dynamic model, O_a is articulation point; O_f and O_r are mass center of front and rear parts, respectively; $x - O_f - y$ is the local coordinate system with coordinate point O_f ; $X - O - Y$ is the global coordinate system;

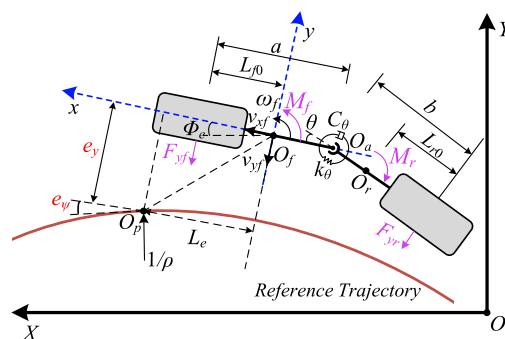


FIGURE 1. Schematic diagram of the vehicle dynamic model.

Based on the analyses above, the lateral and yaw dynamics of DAHVs during steering can be expressed by:

$$\begin{cases} m_f a_{yf} + m_r a_{yr} = F_{yf} + F_{yr} \\ (I_{zf} + m_f (a - L_{f0})^2) \dot{\omega}_f = F_{yf} a + M_f + T_0 \end{cases} \quad (1)$$

where T_0 is the steering torque produced by hydraulic steering system, i.e., $T_0 = k_\theta \theta + C_\theta \dot{\theta}$. a_{yf} and a_{yr} represent the lateral accelerate of front and rear vehicle sections, respectively, which can be expressed by:

$$\begin{cases} a_{yf} = \dot{v}_{yf} + v_x \omega_f \\ a_{yr} = \dot{v}_{yf} + v_x \omega_f - (a - L_{f0} + b - L_{r0}) \dot{\omega}_f + (b - L_{r0}) \ddot{\theta} \end{cases} \quad (2)$$

In this work, a linear tire model is chosen to describe the tire dynamics. Specifically, the lateral forces of the front and rear tires are proportional to the vehicle slip angle. Based on a small slip angle assumption, the lateral tire forces can be simplified as $F_{yf} = 2k_f \alpha_f$, $F_{yr} = 2k_r \alpha_r$, where α_f and α_r are the slip angles in these two sections, which can be formulated as:

$$\begin{cases} \alpha_f = \frac{v_{yf} + L_{f0} \omega_f}{v_{xf}} \\ \alpha_r = \frac{v_{yf} - (a - L_{f0} + b) \omega_f + b \dot{\theta}}{v_{xf}} + \theta \end{cases} \quad (3)$$

The second derivative of the articulation angle is the minimum parameter, which can be ignored in this model. Meanwhile, we define $x_1 = v_{yf}$, $x_2 = \omega_f$, and $x = [x_1, x_2]^T$, and denote the control input as $u = M_f$. The dynamic model of Equation (1) can then be rewritten as:

$$\begin{aligned} \dot{x} &= Ax + Bu + C\dot{\theta} + D\theta \\ &= \begin{bmatrix} a_{11} & a_{12} \\ a_{21} & a_{22} \end{bmatrix} x + \begin{bmatrix} b_1 \\ b_2 \end{bmatrix} u + \begin{bmatrix} c_1 \\ c_2 \end{bmatrix} \dot{\theta} + \begin{bmatrix} d_1 \\ d_2 \end{bmatrix} \theta \end{aligned} \quad (4)$$

where a_{11} , a_{12} , b_1 , c_1 , and d_1 , as shown at the bottom of the page.

Remark: The above analyses provide a dynamic model for DAHVs during steering. Note that this dynamic model contains two active steering effects: hydraulic and skid steering. It can be concluded that if $u = 0$, the dynamic model describes the hydraulic steering process, while $k_\theta = C_\theta = 0$ represents the skid steering process.

Based on this dynamic model, the lateral error and heading error during the vehicle path following process, which is determined by vision dynamics [18], can be described as:

$$\begin{cases} \dot{e}_y = v_{xf} e_\psi - v_{yf} - L_e \omega_f \\ \dot{e}_\psi = v_{xf} \rho - \omega_f \end{cases} \quad (5)$$

Correspondingly, the second derivative of the lateral error and heading error can be expressed by:

$$\begin{cases} \ddot{e}_y = v_{xf} \dot{e}_\psi - \dot{v}_{yf} - L_e \dot{\omega}_f \\ \ddot{e}_\psi = v_{xf} \dot{\rho} - \dot{\omega}_f \end{cases} \quad (6)$$

By combination with Equation (4), Equation (6) can be rewritten as (7), shown at the bottom of the page.

Define $x_{1p} = e_y$, $x_{2p} = e_\psi$, and $x_p = [x_{1p}, x_{2p}]^T$, and denote the control input as $u_p = \theta$. The dynamic model of Equation (7) can then be rewritten as:

$$\ddot{x}_p = A_p \dot{x}_p + C_p x_p + B_p u_p + d_p$$

$$\begin{aligned} &= \begin{bmatrix} a_{11p} & a_{12p} \\ a_{21p} & a_{22p} \end{bmatrix} \dot{x}_p + \begin{bmatrix} c_{11p} & c_{12p} \\ c_{21p} & c_{22p} \end{bmatrix} x_p \\ &+ \begin{bmatrix} b_{1p} \\ b_{2p} \end{bmatrix} u_p + \begin{bmatrix} d_{1p} \\ d_{2p} \end{bmatrix} \end{aligned} \quad (8)$$

where,

$$\begin{aligned} a_{11p} &= a_{11} + a_{21} L_e, \\ a_{12p} &= v_{xf} - a_{11} L_e + a_{12} - a_{21} L_e^2 + a_{22} L_e \\ a_{21p} &= a_{21}, \quad a_{22p} = a_{22} - a_{21} L_e, \quad c_{11p} = 0, \\ c_{12p} &= -a_{11} v_{xf} - a_{21} v_{xf} L_e \\ c_{21p} &= 0, \quad c_{22p} = -a_{21} v_{xf}, \quad b_{1p} = -d_1 - d_2 L_e, \\ b_{2p} &= -d_2 \\ d_{1p} &= (-c_1 - c_2 L_e) \dot{\theta} + (-b_1 - b_2 L_e) M_f \\ &\quad + (a_{11} L_e - a_{12} + a_{21} L_e^2 - a_{22} L_e) v_{xf} \rho \\ d_{2p} &= -c_2 \dot{\theta} - b_2 M_f + (a_{21} L_e - a_{22}) v_{xf} \rho \end{aligned}$$

III. CONTROLLER DESIGN

A. PROBLEM DESCRIPTION

Two controllers are proposed in this paper for path following and skid steering. The objective of the path following controller is to obtain the appropriate steering wheel angle φ for reducing the lateral and heading errors of the vehicle in relation to the reference trajectory. The steering wheel angle is proportionate to the vehicle articulation angle θ , which is controlled by the skid steering method with the direct yaw moment of the front and rear vehicle sections. Due to the different models used by these two control systems, the path-following and skid-steering processes cannot be controlled by a single controller. Therefore, a layered control framework with an upper path following controller and lower skid steering controller is implemented. Among the existing algorithms for the longitudinal or lateral vehicle control, MPC [25] and

$$\begin{cases} a_{11} = \frac{2(k_f + k_r)}{(m_f + m_r)v_x} + \frac{2am_r(a - L_{f0} + b - L_{r0})k_f}{(I_f + m_f(a - L_{f0})^2)(m_f + m_r)v_x}, & a_{21} = \frac{2ak_f}{(I_f + m_f(a - L_{f0})^2)v_x} \\ a_{12} = \frac{2k_f L_{f0} - 2k_r(a - L_{f0} + b)}{(m_f + m_r)v_x} + \frac{2ak_f L_{f0} m_r(a - L_{f0} + b - L_{r0})}{(I_f + m_f(a - L_{f0})^2)(m_f + m_r)v_x} - v_x, & a_{22} = \frac{2ak_f L_{f0}}{(I_f + m_f(a - L_{f0})^2)v_x} \\ b_1 = \frac{m_r(a - L_{f0} + b - L_{r0})}{(I_f + m_f(a - L_{f0})^2)(m_f + m_r)}, & b_2 = \frac{1}{(I_f + m_f(a - L_{f0})^2)} \\ c_1 = \frac{2k_r b}{(m_f + m_r)v_x} + \frac{m_r(a - L_{f0} + b - L_{r0})C_\theta}{(I_f + m_f(a - L_{f0})^2)(m_f + m_r)}, & c_2 = \frac{C_\theta}{(I_f + m_f(a - L_{f0})^2)} \\ d_1 = \frac{2k_r}{(m_f + m_r)} + \frac{m_r(a - L_{f0} + b - L_{r0})k_\theta}{(I_f + m_f(a - L_{f0})^2)(m_f + m_r)}, & d_2 = \frac{k_\theta}{(I_f + m_f(a - L_{f0})^2)} \end{cases}$$

$$\begin{cases} \ddot{e}_y = (v_{xf} - a_{11} L_e + a_{12} - a_{21} L_e^2 + a_{22} L_e) \dot{e}_\psi + (a_{11} + a_{21} L_e) \dot{e}_y + (-a_{11} v_{xf} - a_{21} v_{xf} L_e) e_\psi + \\ \quad + (-d_1 - d_2 L_e) \theta + (-c_1 - c_2 L_e) \dot{\theta} + (-b_1 - b_2 L_e) M_f + (a_{11} L_e - a_{12} + a_{21} L_e^2 - a_{22} L_e) v_{xf} \rho \\ \ddot{e}_\psi = (a_{22} - a_{21} L_e) \dot{e}_\psi + a_{21} \dot{e}_y - a_{21} v_{xf} e_\psi - d_2 \theta - c_2 \dot{\theta} - b_2 M_f + (a_{21} L_e - a_{22}) v_{xf} \rho \end{cases} \quad (7)$$

SMC [26] show growing interest. By contrast, SMC is a nonlinear control approach that has gained much attention for its capacity to deal with disturbance and uncertainty, which is more suitable for the application of the controller design in this paper. Therefore, in order to improve the robustness of the controller, a double sliding mode control (DSMC) method is adopted in the upper and lower controllers. A block diagram of the complete control strategy is shown in Fig. 2.

In this figure, e_p is the tracking deviation, including the lateral and heading errors, which is the input of path following controller with SMC. In this controller, the lateral and heading errors can be reduced by adjusting the steering wheel angle φ , which is the output of the path following controller. e_s is the deviation of the real and referenced articulation angle, which is the input of the skid steering controller with SMC. With this controller, the real articulation angle can be adjusted to the referenced value. Thus, the vehicle can realize the skid steering control. Moreover, v_{xjref} is required vehicle speed. Other parameters in this figure are explained in the following content or in the Appendix A.

B. PATH FOLLOWING CONTROLLER DESIGN

The main idea of an SMC is to drive a closed-loop dynamic system to reach the sliding hyperplane [27]. With reference to the dynamic model expressed by Equation (8), the differential sliding hyperplane is defined as:

$$s = G_e [\dot{e}_p + k_e e_p] \tag{9}$$

where $k_e \in \mathbb{R}^{4 \times 4}$ is an appropriately chosen diagonal matrix with positive diagonal elements. $G_e \in \mathbb{R}^{4 \times 4}$ is a chosen matrix, such that $G_e B_p$ is an identity matrix, which can be defined as $G_e = (B_p^T B_p)^{-1} B_p^T$. $e_p = x_p - x_{ref}$ is the tracking deviation and the desired deviation state is $x_{ref} = 0$. The time derivative of s can be given by:

$$\begin{aligned} \dot{s} &= G_e [\ddot{e}_p + k_e \dot{e}_p] = G_e [\ddot{x}_p + k_e \dot{x}_p] \\ &= G_e A_p \dot{x}_p + G_e C_p x_p + u_p + G_e d_p + G_e k_e \dot{x}_p \end{aligned} \tag{10}$$

Assume that the input of this controller is designed in two parts (considering disturbance or not) and can be denoted as:

$$u_p = u_{no} + u_{nl} \tag{11}$$

where the nominal controller u_{no} is one of the sliding mode controllers that is proposed to provide the desired performance without disturbance. The other additional sliding mode controller u_{nl} is designed to cope with disturbance or model uncertainties. Thus, the controller u_{no} can be defined as:

$$u_{no} = -G_e [(A_p + k_e) \dot{x}_p + C_p x_p] \tag{12}$$

To further solve the controller u_{nl} , the following Lyapunov function is used:

$$V(t) = \frac{1}{2} s^T(t) s(t) \tag{13}$$

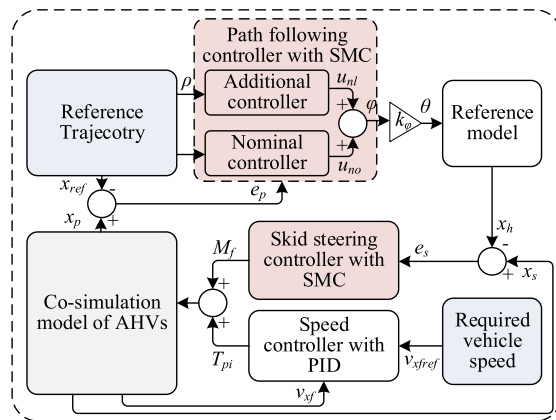


FIGURE 2. Block diagram of the complete control process.

In combination with Equation (9), it can be guaranteed that $V(0) = 0$ and $\dot{V}(t) < 0$ when $s(t) \neq 0$. Therefore, the controller design should satisfy the following equation:

$$\dot{V}(t) = s^T(t) \dot{s}(t) < 0, s(t) \neq 0 \tag{14}$$

Substituting Equations (10)–(12) into Equation (14), the deviation of $V(t)$ can be rewritten as:

$$\begin{aligned} \dot{V}(t) &= s^T [G_e A_p \dot{x}_p + G_e C_p x_p + G_e d_p + G_e k_e \dot{x}_p] \\ &\quad - s^T G_e [(A_p + k_e) \dot{x}_p + C_p x_p] + s^T u_{nl} \\ &= s^T [G_e d_p + u_{nl}] < 0 \end{aligned} \tag{15}$$

To ensure Equation (15) is valid, the controller u_{nl} should be selected as:

$$u_{nl} = -K_p \text{sign}(s) \tag{16}$$

where

$$K_p \geq \|G_e d_p\| \tag{17}$$

where $\|\bullet\|$ is a Hilbert norm.

With the above analyses, it can be concluded that controller u_p can guarantee the dynamic system to reach the sliding hyperplane ($s = 0$). So that the tracking deviation e_p equals 0 within a finite time.

Remark: As a second-order system, the path-following model can be transformed into a first-order system in this controller by designing a differential sliding hyperplane, which can simplify the difficulty of the controller design. Moreover, the curvature of the reference trajectory is regarded as disturbance in this controller design and is compensated by the additional sliding mode controller, which can further improve the precision of path-following process.

C. SKID-STEERING CONTROLLER DESIGN

During skid steering process of DAHVs, the whole hydraulic steering system is removed. So, $k_\theta = C_\theta = 0$. However, due to the independent front and rear vehicle sections, there is one more degree of freedom of control than in a conventional passenger car. One problem should be considered first.

How can we control the direct yaw moment in the front and rear vehicle sections to achieve a certain steering process? This requires revisiting the DAHV steering process with a conventional HSM.

In a DAHV hydraulic steering process, each wheel moves along a trajectory conditioned by the principle of least resistance with the coupled effects of two hydraulic cylinders and one articulation joint. The vehicle articulation angle θ is naturally assigned to the front and rear vehicle sections (θ_f, θ_r and $\theta = \theta_f + \theta_r$). The yaw rates of these two vehicle sections (ω_f and ω_r) can be expressed by:

$$\dot{\theta} = \omega_f - \omega_r \quad (18)$$

This equation demonstrates that the DAHV steering process can be realized by yaw rate control. Meanwhile, by analysis of the vehicle dynamic model in Fig. 1, one can observe that the equivalent steering torque T_0 produced by the HSM is the only active effect during the hydraulic steering process. This is the same in the front and rear vehicle sections. Namely, the appropriate steering torque implemented in the two sections at the same time makes them steer at a certain yaw rate. Correspondingly, the appropriate steering torque can be obtained by the yaw rate control of one vehicle section, which can be then applied to the other section to determine its yaw motion and achieve the overall steering effect. This is the main principle of the proposed skid steering method.

In this subsection, we take the yaw rate of the front vehicle section during a hydraulic steering process as a reference for the design of the skid steering controller. To reduce the influence of the HSM on the skid steering process, the articulation angle θ is replaced by the steering wheel angle φ with coefficient k_φ , denoted by $\theta = k_\varphi \cdot \varphi$. In combination with the vehicle dynamic model (4), the reference yaw rate of the front vehicle section for the skid-steering process can be expressed by:

$$\begin{cases} \dot{x}_h = Ax_h + (C \cdot k_\varphi) \dot{\varphi} + (D \cdot k_\varphi) \varphi \\ y_{sr} = Ex_h \end{cases} \quad (19)$$

where x_h represents the vehicle state during hydraulic steering process; y_{sr} is the reference yaw rate of front vehicle section for DAHVs with skid steering method; $E = \text{diag} [0, 1]$.

In combination with Equation (4), the DAHV dynamic model with SSM can be expressed by:

$$\begin{cases} \dot{x}_s = Ax_s + Bu + d_s \\ y_s = Ex_s \end{cases} \quad (20)$$

where x_s represents the vehicle state during skid steering process; y_s is the real yaw rate of front vehicle section for DAHVs with skid steering method; d_s is the equivalent disturbance $d_s = C_s \dot{\theta} + D_s \theta$, where C_s and D_s are coefficient matrixes, $C_s = [c_1, c_2]^T$, $D_s = [d_1, d_2]^T$, which can be expressed by:

$$\begin{cases} c_1 = \frac{2k_r b}{(m_f + m_r) v_x}, & c_2 = 0 \\ d_1 = \frac{2k_r}{(m_f + m_r)}, & d_2 = 0 \end{cases} \quad (21)$$

Similar to the path following controller design, the SMC method is also used to design the skid-steering controller. The control error is defined as $e_s = x_s - x_h$ and we select the differential sliding hyperplane:

$$s_s(t) = e(t) + k_{se} \int_0^t e(t) dt \quad (22)$$

where k_{se} is weight matrix. Furthermore, the derivation of $s_s(t)$ can be expressed as:

$$\dot{s}_s(t) = \dot{e}_s(t) + k_{se} e_s(t) \quad (23)$$

Substituting Equations (20) and (21) into (23), the derivation of $s_s(t)$ can be rewritten as:

$$\begin{aligned} \dot{s}_s &= \dot{x}_s - \dot{x}_h + k_{se} (x_s - x_h) \\ &= Ax_s + Bu + d_s \\ &\quad - [Ax_h + Ck_\varphi \dot{\varphi} + Dk_\varphi \varphi] + k_{se} (x_s - x_h) \\ &= (A + k_{se}) e + Bu + d_{ss} \end{aligned} \quad (24)$$

where

$$d_{ss} = d_s - Ck_\varphi \dot{\varphi} + Dk_\varphi \varphi \quad (25)$$

To reduce the chattering effect of the SMC, a reaching law with a saturation function and boundary layer is designed as follows:

$$\dot{s}_s = \begin{cases} -\varepsilon \text{sgn}(s_s) & |s_s| > \Delta \\ -\frac{s_s}{\Delta} & |s_s| \leq \Delta \end{cases} \quad (26)$$

where, ε is the coefficient of saturation, and $\varepsilon > 0$; Δ is the boundary layer thickness, and $\Delta > 0$. In combination with Equations (24) and (26), the controller input of the skid steering process can be obtained.

Proof: The Lyapunov function is chosen as:

$$V_s(t) = \frac{1}{2} s_s^T(t) s_s(t) \quad (27)$$

Under the condition of Equation (9), it can be guaranteed that $V_s(0) = 0$ and $V_s(t) > 0$ when $s_s(t) \neq 0$. The derivation of $V_s(t)$ can be expressed by:

$$\dot{V}_s(t) = s_s^T(t) \dot{s}_s(t) \quad (28)$$

When $|s_s| > \Delta$,

$$\dot{V}_s(t) = s_s^T \cdot [-\varepsilon \text{sgn}(s_s)] = -\varepsilon |s_s| < 0 \quad (29)$$

When $|s_s| \leq \Delta$,

$$\dot{V}_s(t) = s_s^T \cdot \left[-\frac{s_s}{\Delta}\right] = -\frac{1}{\Delta} s_s^T s_s < 0 \quad (30)$$

The proof is completed.

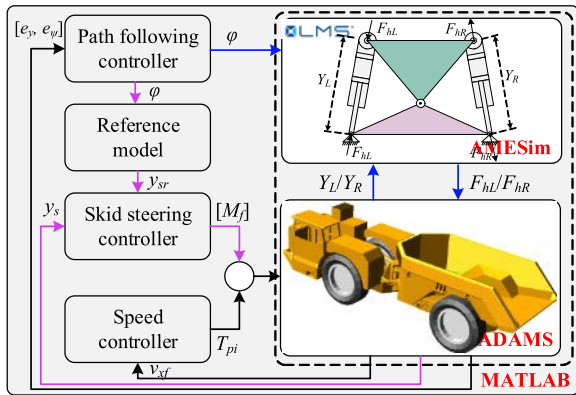


FIGURE 3. Diagram of the co-simulation model.

IV. CASE STUDY

A. VERIFICATION OF DYNAMIC MODELS

In order to verify the proposed controller, a co-simulation model combining ADAMS, AMESim and MATLAB/Simulink was implemented. This verifies the hydraulic steering, skid steering and path following processes of the proposed skid-steering method for DAHVs. A diagram of this co-simulation model is shown in Fig. 3.

In this co-simulation model, vehicle, tire and road models were built in ADAMS while AMESim was used to build a model of the steering unit, hydraulic struts, and accumulator. The pink and blue lines in Fig. 3 represent the controller signals of the vehicle with SSM and HSM, respectively, while the black line represents the vehicle’s common controller signal. With regard to Fig. 3, the steering wheel angle φ is used to control the steering unit of the HSM in AMESim (for hydraulic steering) or to provide the reference vehicle state for the reference model (for skid steering). When it is used to make the simulation for DAHVs with HSM, the data interaction of AMESim and ADAMS can be achieved in MATLAB by transmitting the steering forces F_{hL} and F_{hR} in two hydraulic cylinders with the reference of outputs of cylinders length Y_L and Y_R . The steering forces of the hydraulic cylinders determine the steering process in ADAMS and calculate the new cylinder length, which is input to AMESim for the next step. When the co-simulation model is used to simulate the skid steering process, the skid-steering controller calculates the appropriate direct yaw moment, which is superimposed on the drive wheel to achieve vehicle steering and speed control.

Field tests were also performed with a loaded 35 t DAHV. The experimental area is shown in Fig. 4. The parameters of the vehicle and its HSM can be found in our previous works [8], [9], [28] and is shown in Table. 1 With these parameters, the response comparison of the measure data with simulation results calculated by the dynamic model (with $u = 0$) and co-simulation model are shown in Fig. 5

Combining Fig. 6 from study [29] and FIGURE 5 from the present work, the response comparison of the measured and simulated results show good agreement. The negligible difference reflects the accuracy of these two virtual models.

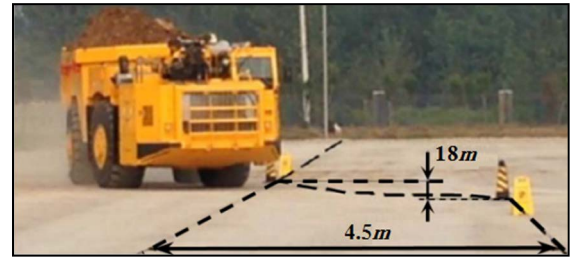


FIGURE 4. DAHV field testing area.

TABLE 1. The parameters of DAHV.

Symbol	Value	Symbol	Value
m_f	21000 kg	k_f	-3000 kN/rad
m_r	52220 kg	k_r	-3500 kN/rad
I_{zf}	31810 kgm ²	a	1710 mm
L_{f0}	386 mm	b	3439 mm
L_{r0}	750 mm	k_{θ}	415070 N/rad

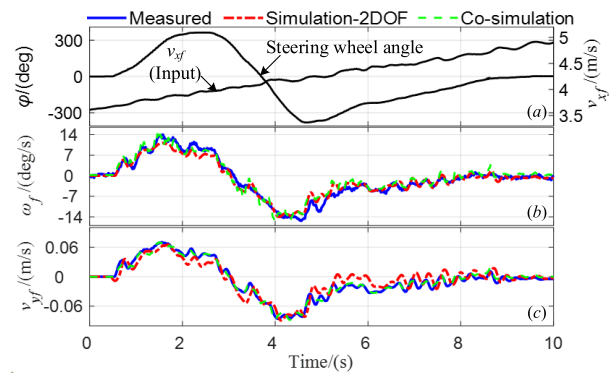


FIGURE 5. Comparison of measured and simulated data. (a) inputs of steering wheel angle and velocity; (b) yaw rate of front vehicle section; (c) lateral velocity of front vehicle section.

B. SIMULATION OF THE DAHV SKID STEERING PROCESS

In this subsection, a co-simulation model is implemented to verify the effectiveness of the DAHV skid-steering controller under ordinary turning driving condition. In the skid steering process, the HSM and two hydraulic cylinders are removed. The vehicle steering process is achieved by the direct yaw moment produced by the differential driving forces of the wheel-side motors. Moreover, in order to highlight the superiority of the proposed skid steering controller based on SMC (denoted as SSM-SMC), a comparative simulation was conducted with a hydraulic steering method (denoted as HSM). Meanwhile, the linear quadratic regulator (LQR) approach (denoted as SSM-LQR), which was proposed for the stability control of DAHVs in previous literature [15], was also used for comparison and to illustrate the importance of the reference model in the skid steering process.

As for the adjustable parameters of DSMC, $k_e = [100, 0; 0, 210]$, $k_{se} = [25, 0; 0, 110]$, $\varepsilon = 0.15$; $\Delta = 0.82$. In the design of LQR, $Q = [330, 0; 0, 31]$, $R = 0.01$.

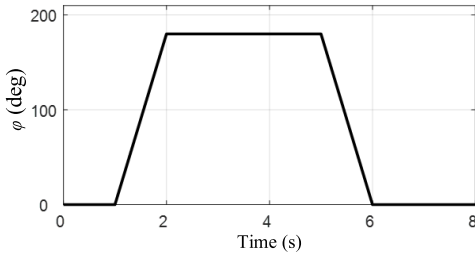


FIGURE 6. Steering wheel angle input in the ordinary turning simulation.

In the simulation, a vehicle was run on a cement road with steering wheel angle input (shown as Fig. 6). Note that the speed of a DAHV is limited under normal working conditions, so the longitudinal vehicle velocity was set to 20 km/h.

The simulated results of the yaw rate ω_f and lateral vehicle velocity v_{yf} of the front vehicle section are shown in Fig. 7. In this figure, ‘Reference’ represents the ideal vehicle state developed by Equation (19). From this figure, one can observe that the HSM, SSM-SMC, and SSM-LQR can all achieve vehicular steering. Compared with HSM, the proposed SSM-SMC shows greater stability and smoothness, especially at the beginning of the steady-state steering process (2 s and 6 s in Fig. 7). Meanwhile, due to oil compression and residual oil pressure in the system [15], the HSM cannot perform the returning function that can be achieved by the SSM-SMC. Moreover, it can also be observed that the SSM-LQR can steer the vehicle with reference to the desired yaw rate when the vehicle is steering in a steady state. However, there still is a large deviation in comparison with the SSM-SMC when the vehicle is in the transient steering process at 1–2 s. This deviation causes a large response lag in the vehicle articulation angle, as shown in Fig. 8.

The simulated yaw rate of the rear vehicle section ω_r and vehicle articulation angle θ are shown in Fig. 8. It shows that the steering of the rear section can also be controlled by the same direct yaw moment applied to the front section via the SMC control method. The yaw rate of the rear section with SSM-SMC shows smoother and more stable than with HSM. Although the state of the rear section controlled by SSM-LQR is smoother than those of SSM-SMC and HSM, there is a large steering lag for the rear section, which causes the vehicle articulation angle to fail to track the desired value. With the further analysis of vehicle articulation angle shown in Fig. 8, the oscillating vehicle state under HSM causes the vehicle to steer unstably. The HSM cannot return the articulation angle to 0 at the end of the steering process, as concluded above.

In order to further verify the effectiveness of the proposed control method, a double-lane change driving condition is implemented to make simulation when the vehicle speed is 35km/h. As shown in Fig. 9, the input of steering wheel angle is setting at 1s and the maximum value is 180 deg. With the input of this condition, the results of the yaw rate and lateral velocity of front vehicle section are shown in Fig.10.

It can be found from Fig. 10 that the yaw rate of front vehicle section tracks the reference well while the error of

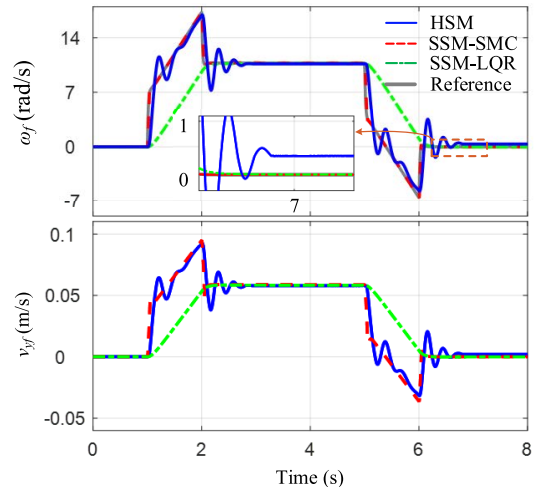


FIGURE 7. Vehicle states in the ordinary turning simulation.

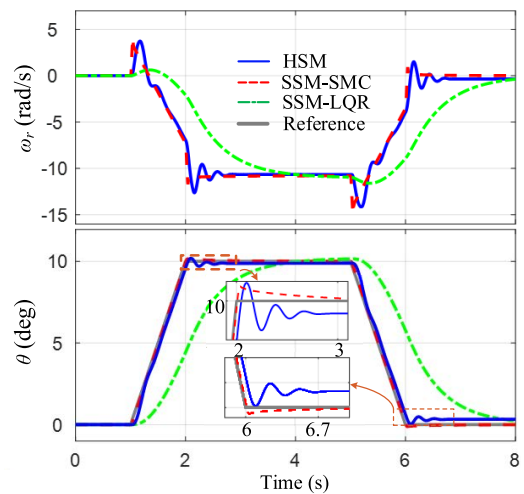


FIGURE 8. Vehicle dynamic parameters in the ordinary turning simulation.

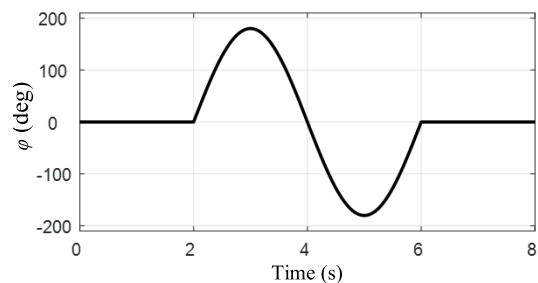


FIGURE 9. Steering wheel angle input under the double-lane change.

lateral velocity is maintained in the reasonable region during skid steering process. With the comparison with HSM, the SSM-SMC can steer DAHVs with smooth and stable yaw rate and lateral velocity. Note that the deviations of the yaw rate of front vehicle section during hydraulic steering process at the end of simulation is much less than that in the ordinary turning condition. That is because of the counteraction of the deviations when the vehicle turns to different directions, which has been introduced in the Section II.

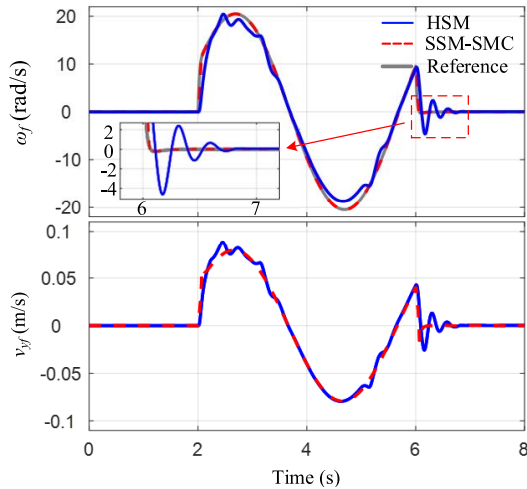


FIGURE 10. Results of the vehicle states in the double-lane change simulation.

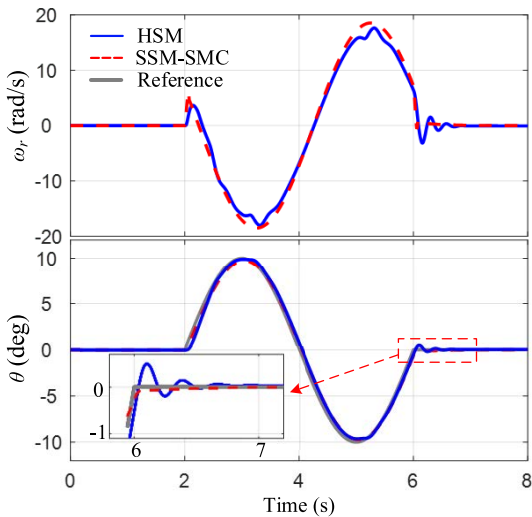


FIGURE 11. Results of the vehicle dynamic parameters in the double-lane change simulation.

Fig.11 shows the simulation results of yaw rate in rear vehicle section and the vehicle articulation angle in double-lanes change driving condition. From the simulation results, one can observe that, the yaw rate of rear vehicle section in SSM has smaller fluctuations than that in HSM. And the vehicle articulation angle does have the correct response according to the steering wheel angle input and can successfully accomplish the double-lanes change manoeuvre.

In conclusion, reasonable control of the direct yaw moment of the front and rear vehicle sections allows DAHVs to steer more stability and smoothness than with a conventional hydraulic steering method.

C. SIMULATION OF THE PATH FOLLOWING PROCESS FOR DAHVs WITH SKID STEERING

In this subsection, we simulate path-following control for DAHVs using the skid steering method to verify the proposed

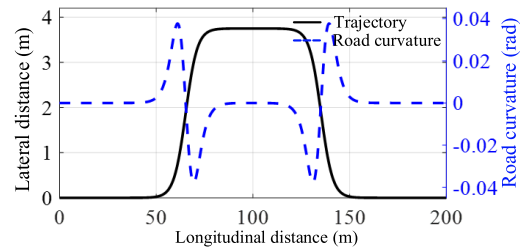


FIGURE 12. Reference trajectory and road curvature in the path-following simulation.

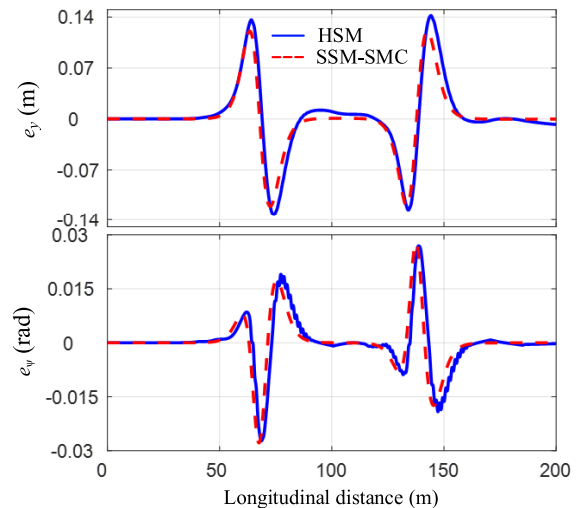


FIGURE 13. Lateral and heading errors in the path-following simulation.

controller. The reference trajectory and road curvature used in the simulation are shown in Fig. 12.

With the reference trajectory design, the path following process of DAHVs was simulated using different steering methods. Its lateral error and heading error are shown in Fig. 13. From this figure, one can observe that both HSM and SSM-SMC can achieve path following control of DAHVs, with the greatest lateral and heading errors are less than 0.15 m and 0.03 rad, respectively. Comparison of these two control methods indicates that SSM-SMC can improve steering stability and vehicle smoothness by improving the accuracy of the path following control process. Moreover, because the vehicle section of DAHV cannot return back (the vehicle articulation angle cannot return to 0 when the steering wheel angle returns to 0, as discussed previously), there are errors when the vehicle is run in a straight line. By contrast, the SSM-SMC solves this problem well and further improves the path following control accuracy.

The steering wheel angle and driving torque of the different wheels during path following are shown in Fig. 14. It shows that the steering wheel angle input under SSM-SMC is smoother than that under HSM. This is also true for straight-line driving. Moreover, during a skid steering process, the direct yaw moment is distributed to both the inside

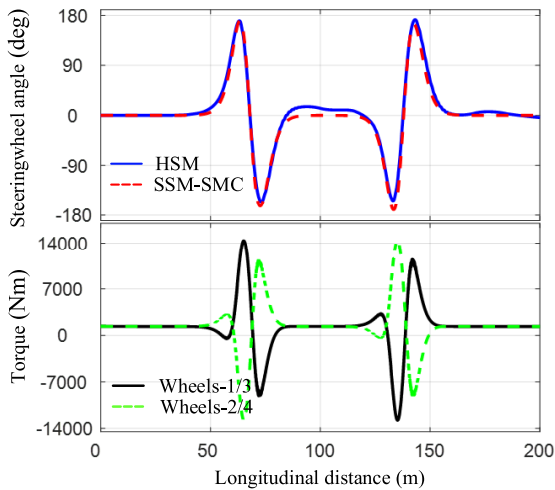


FIGURE 14. Control inputs of steering-wheel angle and driving torque at different wheels.

and outside wheels of the front and rear vehicle sections, and is added to the driving torque that maintains the longitudinal velocity.

In conclusion, the skid steering method improves the steering performance and path-following control accuracy of DAHVs on the basis of simplifying the vehicle structure.

V. CONCLUSION

In this paper, a novel skid steering method and a layered control framework consisting of an upper path following controller and lower steering controller were developed for DAHVs. The SSM was utilized to be the sole power source to replace the conventional HSM to improve vehicle steering performance on the basis of simplifying the vehicle structure. Double SMC techniques were implemented to realize steering and path following control of DAHVs with improved control system robustness and path following control accuracy. Finally, a co-simulation model tested by field tests was used to verify the effectiveness of the proposed control methods. The following conclusions can be drawn.

1) The SSM-SMC approach proposed in this paper can replace the conventional HSM and significantly improve the steady- and transient-state steering performance of DAHVs relative to what is possible with an HSM or SSM-LQR.

2) The proposed layered control framework with DSMC provides satisfactory path following performance and has lower lateral and heading errors and smoother steering wheel angle responses than those of a conventional HSM.

In future work, the path following performance and steering response characteristics of different steering methods will be considered for comparison and to verify the advantages of using SSMs in DAHVs. Furthermore, field tests with real vehicles will be conducted to verify the effectiveness of the proposed control paradigm.

APPENDIX A

Notation	Definition
a	The distance between front wheel axle and articulation joint
a_{yf}	Lateral accelerate of front vehicle sections
a_{yr}	Lateral accelerate of rear vehicle sections
b	The distance between rear wheel axle and articulation joint
m_f	Mass of front parts of the vehicle
m_r	Mass of rear parts of the vehicle
I_{zf}	Inertia moment through the centre of gravity in front vehicle section
T_0	The steering torque produced by hydraulic steering system
C_θ	The damping of the equivalent hydraulic steering system
k_θ	The stiffness of the equivalent hydraulic steering system
e_y	Lateral error
e_ψ	Heading error
F_{yf}	The lateral tire forces in front vehicle section
F_{yr}	The lateral tire forces in rear vehicle section
k_f	The cornering stiffness of tires in front vehicle section
k_r	The cornering stiffness of tires in rear vehicle section
L_e	Preview distance
L_{f0}	The distance from mass center of front vehicle section to the front axle
L_{r0}	The distance from mass center of rear vehicle section to the rear axle
M_f	The direct yaw moment produced by the differential longitudinal tire forces of two wheel-side motors in front vehicle section
M_r	The direct yaw moment produced by the differential longitudinal tire forces of two wheel-side motors in rear vehicle section
v_{xf}	The longitudinal vehicle velocity
v_{yf}	The lateral vehicle velocity
α_f	The slip angle of tires in front vehicle section
α_r	The slip angle of tires in rear vehicle section
ω_f	Yaw rate of front vehicle section
θ	The vehicle articulation angle
ρ	Path curvature
DAHVs	Distributed-drive articulated heavy vehicles
DSMC	double sliding mode control
HSM	hydraulic steering method
SSM	skid-steering method
SMC	sliding mode control
NMPC	non-linear model predictive control
LQR	linear quadratic regulator

REFERENCES

[1] T. Xu, Y. Liu, X. Cao, and X. Ji, "Cascaded steering control paradigm for the lateral automation of heavy commercial vehicles," *IEEE Trans. Transp. Electric.*, early access, Dec. 8, 2021, doi: 10.1109/TTE.2021.3134023.

- [2] U. Montanaro, S. Dixit, S. Fallah, M. Dianati, A. Stevens, D. Oxtoby, and A. Mouzakitis, "Towards connected autonomous driving: Review of use-cases," *Vehicle Syst. Dyn.*, vol. 57, no. 6, pp. 779–814, 2018.
- [3] K. P. Divakarla, A. Emadi, and S. Razavi, "A cognitive advanced driver assistance systems architecture for autonomous-capable electrified vehicles," *IEEE Trans. Transport. Electric.*, vol. 5, no. 1, pp. 48–58, Mar. 2019.
- [4] Y. Gao, D. Cao, and Y. Shen, "Path-following control by dynamic virtual terrain field for articulated steer vehicles," *Vehicle Syst. Dyn.*, vol. 58, no. 10, pp. 1528–1552, 2019.
- [5] Q. Gu, L. Liu, G. Bai, K. Li, Y. Meng, and F. Ma, "Longitudinal and lateral trajectory planning for the typical duty cycle of autonomous load haul dump," *IEEE Access*, vol. 7, pp. 126679–126695, 2019.
- [6] Y. Gao, Y. Ai, B. Tian, L. Chen, J. Wang, D. Cao, and F.-Y. Wang, "Parallel end-to-end autonomous mining: An IoT-oriented approach," *IEEE Internet Things J.*, vol. 7, no. 2, pp. 1011–1023, Feb. 2020.
- [7] T. Berglund, A. Brodnik, H. Jonsson, M. Staffanson, and I. Söderkvist, "Planning smooth and obstacle-avoiding B-spline paths for autonomous mining vehicles," *IEEE Trans. Autom. Sci. Eng.*, vol. 7, no. 1, pp. 167–172, Jan. 2010.
- [8] T. Xu, Y. Shen, Y. Huang, and A. Khajepour, "Study of hydraulic steering process for articulated heavy vehicles based on the principle of the least resistance," *IEEE/ASME Trans. Mechatronics*, vol. 24, no. 4, pp. 1662–1673, Aug. 2019.
- [9] T. Xu, X. Ji, and Y. Shen, "A novel assist-steering method with direct yaw moment for distributed-drive articulated heavy vehicle," *Proc. Inst. Mech. Eng., K, J. Multi-Body Dyn.*, vol. 234, no. 1, pp. 214–224, Mar. 2020.
- [10] T. Nayl, G. Nikolakopoulos, T. Gustafsson, D. Kominiak, and R. Nyberg, "Design and experimental evaluation of a novel sliding mode controller for an articulated vehicle," *Robot. Auto. Syst.*, vol. 103, pp. 213–221, May 2018.
- [11] Y. He, A. Khajepour, J. McPhee, and X. Wang, "Dynamic modelling and stability analysis of articulated frame steer vehicles," *Int. J. Heavy Veh. Syst.*, vol. 12, no. 1, pp. 28–59, 2004.
- [12] N. L. Azad, A. Khajepour, and J. McPhee, "Effects of locking differentials on the snaking behaviour of articulated steer vehicles," *Int. J. Veh. Syst. Model. Test.*, vol. 2, no. 2, pp. 101–127, 2007.
- [13] C. Jin, P. Wang, Y. Shen, and B. Jossey, "Differential control strategy based on an equal slip rate for an all-wheel electric-drive underground articulated dumping truck," *J. Eng. Sci. Technol. Rev.*, vol. 4, no. 7, pp. 163–168, 2014.
- [14] Y. Yin, S. Rakheja, and P.-E. Boileau, "Multi-performance analyses and design optimisation of hydro-pneumatic suspension system for an articulated frame-steered vehicle," *Vehicle Syst. Dyn.*, vol. 57, no. 1, pp. 108–133, 2019.
- [15] Y. Gao, Y. Shen, T. Xu, W. Zhang, and L. Guvenc, "Oscillatory yaw motion control for hydraulic power steering articulated vehicles considering the influence of varying bulk modulus," *IEEE Trans. Control Syst. Technol.*, vol. 27, no. 3, pp. 1284–1292, May 2019.
- [16] M. Iida, H. Nakashima, H. Tomiyama, T. Oh, and T. Nakamura, "Small-radius turning performance of an articulated vehicle by direct yaw moment control," *Comput. Electron. Agricult.*, vol. 76, no. 2, pp. 277–283, May 2011.
- [17] C.-L. Hwang, C.-C. Yang, and J. Y. Hung, "Path tracking of an autonomous ground vehicle with different payloads by hierarchical improved fuzzy dynamic sliding-mode control," *IEEE Trans. Fuzzy Syst.*, vol. 26, no. 2, pp. 899–914, Apr. 2018.
- [18] J. Guo, L. Li, K. Li, and R. Wang, "An adaptive fuzzy-sliding lateral control strategy of automated vehicles based on vision navigation," *Vehicle Syst. Dyn.*, vol. 51, no. 10, pp. 1502–1517, Jun. 2013.
- [19] P. Nilsson, L. Laine, and B. Jacobson, "A simulator study comparing characteristics of manual and automated driving during lane changes of long combination vehicles," *IEEE Trans. Intell. Transp. Syst.*, vol. 18, no. 9, pp. 2514–2524, Sep. 2017.
- [20] L. Zhang, Z. Wang, X. Ding, S. Li, and Z. Wang, "Fault-tolerant control for intelligent electrified vehicles against front wheel steering angle sensor faults during trajectory tracking," *IEEE Access*, vol. 9, pp. 65174–65186, 2021.
- [21] Y. Liu, X. Ji, K. Yang, X. He, X. Na, and Y. Liu, "Finite-time optimized robust control with adaptive state estimation algorithm for autonomous heavy vehicle," *Mech. Syst. Signal Process.*, vol. 139, May 2020, Art. no. 106616.
- [22] A. Astolfi, P. Bolzern, and A. Locatelli, "Path-tracking of a tractor-trailer vehicle via Lyapunov techniques," in *Proc. Eur. Control Conf. (ECC)*, Sep. 2001, pp. 451–456.
- [23] T. Nayl, G. Nikolakopoulos, and T. Gustafsson, "A full error dynamics switching modeling and control scheme for an articulated vehicle," *Int. J. Control, Autom. Syst.*, vol. 13, no. 5, pp. 1221–1232, Oct. 2015.
- [24] N. L. Azad, A. Khajepour, and J. McPhee, "Robust state feedback stabilization of articulated steer vehicles," *Vehicle Syst. Dyn.*, vol. 45, no. 3, pp. 249–275, 2007.
- [25] D. Tavernini, M. Metzler, P. Gruber, and A. Sorniotti, "Explicit nonlinear model predictive control for electric vehicle traction control," *IEEE Trans. Control Syst. Technol.*, vol. 27, no. 4, pp. 1438–1451, Jul. 2019.
- [26] X. Ding, Z. Wang, and L. Zhang, "Hybrid control-based acceleration slip regulation for four-wheel-independent-actuated electric vehicles," *IEEE Trans. Transport. Electric.*, vol. 7, no. 3, pp. 1976–1989, Sep. 2021.
- [27] Y. Zheng, J. Liu, X. Liu, D. Fang, and L. Wu, "Adaptive second-order sliding mode control design for a class of nonlinear systems with unknown input," *Math. Problems Eng.*, vol. 2015, Oct. 2015, Art. no. 319495.
- [28] T. Xu, X. Ji, Y. Liu, and Y. Liu, "Differential drive based yaw stabilization using MPC for distributed-drive articulated heavy vehicle," *IEEE Access*, vol. 8, pp. 104052–104062, 2020.
- [29] T. Xu, X. Ji, C. Fei, Y. Liu, and Y. Shen, "Research on assist-steering method for distributed-drive articulated heavy vehicle based on the co-simulation model," SAE Tech. Paper 2020-01-0761, 2020.



FANG YANG received the B.S. and Ph.D. degrees from Southwest University, China, in 2019. She is currently a Postdoctoral Researcher in applied economics and economics with the Postdoctoral Research Center of Agricultural Bank of China. Her main research interests include digital economy and intelligent agriculture.



XUANHAO CAO received the B.S. degree from Jilin University, Changchun, China, in 2017, where he is currently pursuing the Ph.D. degree in control science and engineering. He is also jointly training doctoral students with the State Key Laboratory of Automotive Safety and Energy, Tsinghua University, Beijing, China. His main research interest includes intelligent vehicle modeling and control.



TAO XU received the B.S. degree in vehicle engineering from the Shandong University of Science and Technology, Shandong Province of China, in 2013, and the Ph.D. degree in mechanical engineering from the University of Science and Technology Beijing, China, in 2019. He is currently a Postdoctoral Researcher of vehicle engineering with Tsinghua University. His research interests include heavy vehicle design and control, and vehicle dynamics and control.



XUEWU JI received the B.S., M.S., and Ph.D. degrees in automotive engineering from the College of Automotive Engineering, Jilin University, China, in 1987, 1990, and 1994, respectively. He is currently an Associate Professor with the State Key Laboratory of Automotive Safety and Energy, Tsinghua University, China. His research interests include vehicle dynamics and control and advanced steering system technology. He received the National Science and Technology Progress

Award for his achievements in the industrialization of electric power steering technology, in 2014.

...